# Two Semi-Active Approaches for Vibration Isolation: Piezoelectric Friction Damper and Magnetorheological Damper

M. Unsal, C. Niezrecki, C. Crane III
*Department of Mechanical and Aerospace Engineering, University of Florida, Gainesville, Florida, 32611-6250*

## Abstract

*Two different approaches to perform vibration isolation control on a single-degree-of-freedom system using semi-active dampers are investigated. In the first approach, the friction damper consists of an actuator, which is based on a piezoelectric stack with a mechanical amplifying mechanism that provides symmetric forces within the isolator. The advantages of such an actuator are its high bandwidth, displacement response and its ability to operate in vacuum environments such as in space. The damper is constrained to move using an air bearing that produces a virtually ideal single-degree-of-freedom spring-mass system. Within this work, the actuating ability of the friction-based actuator is characterized. The relationship between the force generated by the actuator and the applied voltage was found to be linear. In the second approach, a magnetorheological (MR) fluid damper is designed and fabricated. This damper is ideal for use in a semi-active control system where the damping characteristics can be adjusted by varying the amount of current applied to the damper.*

## 1. Introduction

Semi-active control has been developed as a compromise between passive and active control. Instead of opposing a primary disturbance as is the case with active control, semi-active control scheme applies a secondary force to the system. Semi-active control has recently been an area of much interest because of its potential to provide the adaptability of active devices without requiring a significant external power supply for actuators. A semi-active control system cannot provide energy to a system comprising the structure and actuator, but it can achieve favorable results by altering the properties of the system, such as stiffness and damping [1]. Unlike an active system, the control forces developed are related to the motion of the structure. Furthermore, the stability of the semi-active system is guaranteed as the control forces typically oppose the motion of the structure [2].

The need for vibration isolation is becoming increasingly important for precision structures and sensitive high technology equipment. More reliable devices with a higher bandwidth, smaller size, and lower power requirement are needed. Semi-active control of vibration isolation is an area of much interest due to its potential to provide these characteristics. This paper focuses on the development of two different semi-active dampers to be used in a vibration isolation system.

### 1.1 Piezoelectric friction damper

Friction damping has long been used as an effective and simple method to add passive damping to mechanical systems. It requires only the direct contact of two parts moving relative to each other and it can be incorporated into harsh environments and vacuum environments where the use of elastomeric damping treatments and fluid filled dampers is limited [3]. Ferri and Heck first came up with the idea of varying the normal force in a frictional joint to enhance energy dissipation from a vibrating structure [4]. A semi-active friction damper feeds back an actuation force to the mechanical system whose dynamics can be altered in this way. The properties of the system, such as stiffness and damping can be actively changed through the control of this actuation force.

The development of friction dampers to the extent of other semi-active dampers has been impeded due to three primary reasons. First of all, because of the discontinuity of friction at zero velocity, the differential equation of motion of the dynamic system is dependent on the direction of velocity [3]. Secondly, when the static coefficient of friction is noticeably greater than the kinetic coefficient, the "stick-slip" phenomenon occurs. This phenomenon is caused by the fact that the friction force does not remain constant as a function of some other variable, such as temperature, displacement, time, or velocity. For the two reasons stated, friction dampers are non-linear and will require a non-linear controller. The third and most important reason friction dampers have not been fully developed is due to the actuator. In past research, the normal force was altered through the use of hydraulics [5]. The main disadvantage of hydraulics is the time delay that is required for the actuator to reach the required pressure. Rapid modulation of the actuation force is not possible and it could cause a backlash effect when used. In a variable friction damper system, the speed with which the actuation force can be adjusted is of utmost importance [6]. Modern electromagnetic actuators are well suited to provide rotational motion (electric motors); however, their use as linear actuators is limited. Although they are capable of generating sufficient force and displacement, the large size, weight, electrical demands, and cost of these actuators make them currently impractical. Recently, piezoelectric actuators have been

proposed as a method of applying the varying normal force [6, 7]. Piezoelectricity is the ability of certain crystalline materials to develop an electric charge proportional to a mechanical stress and vice versa. Piezoelectric materials can generate a significant amount of stress/strain in a constrained condition when exposed to an electric field. This property has been used to suppress excessive vibration of mechanical and aerospace systems and is still an active area of research [6]. Due to their high force and bandwidth capability, piezoelectric actuators appear to be a natural candidate for use in friction dampers. However until only recently, the maximum (freely loaded) mechanical strain of these devices did not exceed 0.1%. This means that an actuator 1 inch long could only deflect 0.001 inch (significantly less under load). As a result, the development of a practical frictional damper has been hampered.

A flextensional piezoelectric amplifier (using an ordinary piezoelectric material) has recently been developed (FPA-1700, Dynamic Structures and Materials, LLC) that can generate a 1.6 mm displacement having a load of 10 lbs. This specific actuator was chosen to be implemented in the developed vibration isolator due to its high displacement capability and also due to the inherent characteristics of piezoelectric actuators, which make them favorable when compared with other actuators. They have the potential to be effective over a wide frequency range with high-speed actuation, low power consumption, reliability and compactness.

Within this work, a novel semi-active friction damper is created. The actuating ability of the damper is quantified through an experiment. This damper has potential application to space environments in which other viscous dampers are not suitable. It may also have application to civil engineering structures, parallel platform mechanisms, large space structures, and vehicle suspensions.

## 1.2 Magnetorheological damper

The robustness and the simple mechanical design of magnetorheological (MR) dampers make them a natural candidate for a semi-active control device. They require minimal power while delivering high forces suitable for full-scale applications. They are fail-safe since they behave as passive devices in case of a power loss [8]. MR fluids are suspensions of small iron particles in a base fluid. They are able to reversibly change from free-flowing, linear viscous liquids to semi-solids having controllable yield strength under a magnetic field. When the fluid is exposed to a magnetic field, the particles form linear chains parallel to the applied field as shown in Fig. 1. These chains impede the flow and solidify the fluid in a matter of milliseconds. This phenomenon develops a yield stress which increases as the magnitude of the applied magnetic field increases [9].

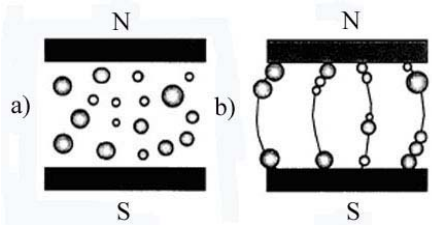


**Fig. 1. Magnetorheological fluid: a) no magnetic field, b) with magnetic field [9]**

MR devices can be divided into three groups of operational modes or a combination of the three based on the design of the device components. In the valve mode, of the two surfaces that are in contact with the MR fluid, one surface moves relative to the fluid. This relative motion creates a shear stress in the fluid. The shear strength of the fluid may be varied by applying different levels of magnetic field. In the direct shear mode, the fluid is pressurized to flow between two surfaces which are stationary. The flow rate and the pressure of the fluid may be adjusted by varying the magnetic field. In the squeeze film mode, two parallel surfaces squeeze the fluid in between and the motion of the fluid is perpendicular to that of the surfaces. The applied magnetic field determines the force needed to squeeze the fluid and also the speed of the parallel surfaces during the squeezing motion [10].

A magnetic circuit is necessary to induce the changes in the viscosity of the MR fluid. By using Kirchoffs's Law of magnetic circuits, the necessary number of amp-turns (*NI*) is

$$NI = \sum H_i L_i = H_f g + H_s L \qquad (1)$$

where $H_f$ and $H_s$ are the magnetic field intensity of the fluid and the steel, respectively, g is the length of the gap where the fluid flows, and L is the total length of the steel path. From (1), it is clear that, to increase the total magnetic field intensity, the number of amp-turns have to be kept at a maximum while minimizing the length of the fluid gap and the steel path. However, sufficient cross-section of steel must be maintained such that the magnetic field intensity in the steel is very low. Also, too small a fluid gap would cause the damping force to be too high when no magnetic field is applied. The magnetic circuit typically uses low carbon steel, which has a high magnetic permeability and saturation. This steel effectively directs magnetic flux into the fluid gap.

Several different designs of MR dampers have been built and tested in the past. The first of these designs is the bypass damper, shown in Fig. 2a), where the bypass flow occurs outside the cylinder and an electromagnet applies a magnetic field to the bypass duct [11]. While this design has a clear advantage that the MR fluid is not directly affected by the heat build-up in the electromagnet, the presence of the bypass duct makes it a less compact design.

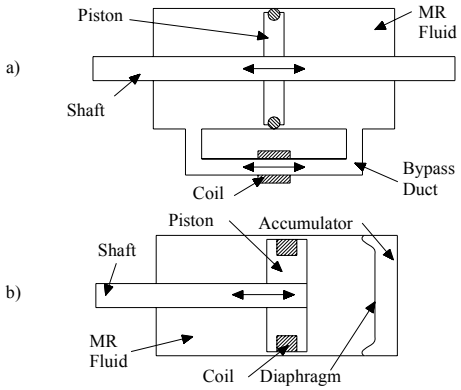


**Fig. 2. Schematic of a) MR fluid bypass damper b) MR fluid damper with accumulator**

In another design by Lord Corporation, the electromagnet is inside the cylinder and the MR fluid passes through an annular gap around the electromagnet as shown in Fig. 2b). This design uses an accumulator to make up for the volume of fluid displaced by the piston rod which is going into the damper [12]. A way to get rid of this accumulator and simplify the design is to build a double-shafted damper [13]. However, most of these dampers were intended for large-scale applications such as vibration isolation of buildings and bridges. A linear, double-shaft MR damper with the electromagnet placed inside the cylinder is the focus of this research. This MR damper will have a lower minimum damping force suitable for small-scale applications and is intended for use with parallel platform mechanisms where a damper will adjust the damping in each leg connector of the mechanism.

## 2. Theoretical modeling

### 2.1 Friction damping

The forces acting on the moving mass of the system are the spring force, the friction force and the external force applied by the shaker. The sum of these forces provides the inertial force.

Therefore,

$$\sum F = m\ddot{x} = -F_{spring} - F_{friction} + F_{external}. \qquad (2)$$

The acceleration and the applied external force are measured using an accelerometer and a force transducer, respectively. While for the system identification experiments, the spring is included in the damper, it is removed from the system for the friction force experiments. Therefore, by rearranging (2) and taking out the spring force, it is possible to measure the friction force generated by the actuator.

Therefore, the friction is given by,

$$F_{friction} = F_{external} - m\ddot{x}. \qquad (3)$$

Equation (3) is used to quantify the performance of the new semi-active friction damper. The acceleration and the external force are measured in order to compute the frictional force capabilities of the damper.

### 2.2. MR fluids

The Bingham plastic model which is an extension of the Newtonian flow is often used to describe the behavior of MR fluids. It is obtained by also taking into account the yield stress of the fluid. The flow is assumed to occur when the dynamic yield stress is reached. The total stress is given by

$$\tau = \tau_y \,\mathrm{sgn}(\dot{\gamma}) + \eta\dot{\gamma} \qquad (4)$$

where $\tau_y$ is the yield stress induced by the magnetic field, $\dot{\gamma}$ is the shear rate and $\eta$ is the viscosity of the fluid. Stanway, *et al.* came up with an idealized mechanical model based on this model which has a Coulomb friction element in parallel with a viscous damper [13]. In this model, for nonzero piston velocities, the force generated is given by

$$F = f_c \,\mathrm{sgn}(\dot{x}) + c_o\dot{x} \qquad (5)$$

where $c_o$ is the damping coefficient and $f_c$ is the frictional force, which is related to the fluid yield stress [14]. In the post-yield part, the slope of the force-velocity curve is equal to the damping coefficient which is essentially the viscosity of the fluid, $\eta$, as shown in Fig. 3. The idealized model force vs. velocity behavior is represented by a dashed line, while the actual damper behavior is represented by a solid line.

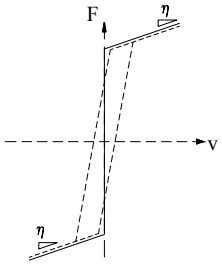


**Fig. 3. Schematic of the Bingham model [14].**

## 3. Experimental Setup

### 3.1. Piezoelectric friction damper

The actuator that is used within this work is the FPA-1700 Low Voltage Piezoelectric Actuator by Dynamic Structures &

Materials, LLC and is shown in Fig. 4. The actuator incorporates a shape memory alloy preload wire for bi-directional motion and a titanium flexure-based amplification mechanism. The peak output stroke of the actuator when it is not loaded is approximately 1.6 mm. The displacement of the mechanism is transmitted through two parallel output plates. The friction pads are kevlar bike disc brake pads (CODA QPDPAD/BLU) and the housing is stainless steel.

The friction damper in this work consists of several moving and stationary components as shown in Fig. 5. A 0.75" diameter shaft is fixed to the base of the damper. Mounted to the shaft is the flextensional mechanical amplifier of the piezoelectric actuator. The moving components consist of the outer housing and the air bearing. The outer housing also comes in contact with the friction pads as it vibrates. The friction pads are fixed to both sides of the actuator so that the normal force that the actuator applies is symmetrical. The normal force provided between the friction pads and the outer housing induces a frictional load, which retards the motion of the outer housing. Within this damper, there is also a spring, which connects the moving housing to the stationary base. With the frictional pads not engaged, the air bearing provides a relatively frictionless contact surface. As a result, the damper is essentially an ideal SDOF system. The mass of the moving elements is 1.690 kg and the natural frequency is 5.23 Hz.

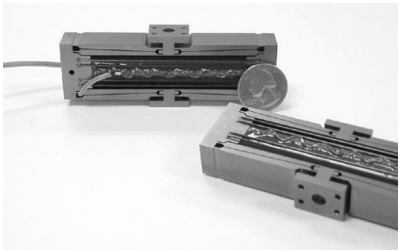

**Fig. 4. FPA-1700-LV piezoelectric actuator**

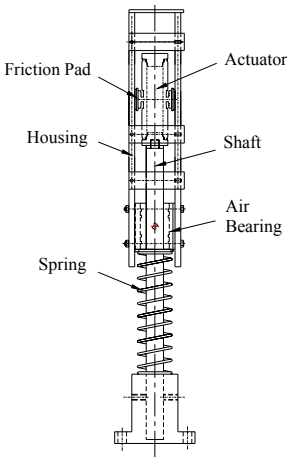


**Fig. 5. Friction damper (front view)**

The vibration isolator has been designed so that the friction damper is fixed horizontally as shown in Fig. 6. The base of the friction damper is screwed onto a vertical steel plate and the moving outer housing is connected to the shaker through the force transducer and the stinger. The shaker is bolted onto two steel plates. It is positioned so that the friction damper's line of symmetry is in line with the central fixing hole of the shaker. The accelerometers are fixed to the outer housing using wax. The stroke of vibration is 12.0 mm. The signals from all the transducers are fed to the DSPT SigLab (20-42) analyzer through the signal conditioner, model 482A16 from PCB Piezoelectronics. The shaker input signal is generated with the SigLab analyzer. The normal force controller is designed in Simulink, a MATLAB plug-in, and implemented in real-time through dSPACE. The actuator input signal is generated in dSPACE and output through the digital-to-analog converter (DAC) as shown in Fig. 7.

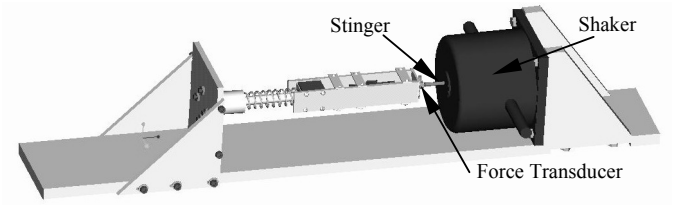


**Fig. 6. Friction damper with shaker and transducers (3D view)**

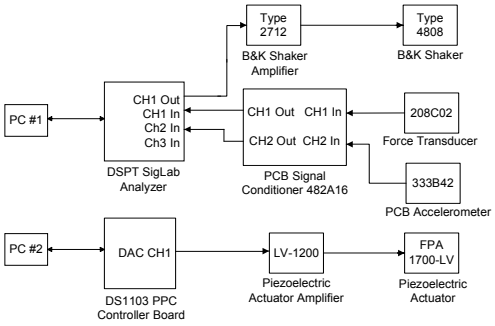


**Fig. 7. Schematic drawing of the experimental setup**

## 3.2. MR damper

The MR damper utilizes the unique properties of the MR fluid. In this design, the MR fluid flows through the annular gap between the housing and the magnetic body as seen in Fig. 8. The damper operates in a combination of valve and direct shear modes. A magnetic field is created along this gap through the use of a coil which is wrapped around the magnetic body. When the magnetic field is applied, the viscosity of the magnetorheological fluid increases in a matter of milliseconds. The field causes a resistance to the flow of fluid between the two reservoirs. This way, the damping

coefficient of the damper is adjusted. Therefore, the damping coefficient of the damper can be adjusted by feeding back a conditioned sensor signal to the coil.

All the parts of this damper were manufactured from low-carbon steel which has a high magnetic permeability. The magnetic body was designed to divide the coil into two parts which creates three effective magnetic surfaces. The two coils were wound in directions opposite to each other so that the flux lines would add up in the middle, as shown in Fig. 8. The flux lines are perpendicular to the flow of the MR fluid. To increase the total magnetic field intensity, the length of the steel path and the fluid path were kept at a minimum. The thickness of the housing is 4.75 mm. The annular gap between the magnetic body and the housing is 0.030 mm.
The total length of the damper, shown in Fig. 9 is 220 mm, while its stroke is 62 mm.

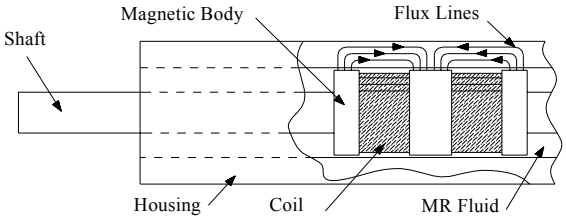


**Fig. 8. Schematic of the double-shaft MR damper**

**Fig. 9. Double-shaft MR damper made from low-carbon steel**

## 4. Results

Several experiments are carried out in order to characterize the friction force capability of the novel piezoelectric-based isolator. For these experiments, the friction pads are in contact with the outer housing and the spring is removed. Therefore, the difference between the input force and the inertial force yields the friction force induced by the actuator. The results of the experiments for a shaker input voltage of 9 V, excitation frequency of 20 Hz and actuator input voltage of 30 V are displayed in Fig. 10. This graph is representative of typical results for the many different test cases measured. Tests were conducted for several different actuator input voltages (30, 60, 90, and 120 V), excitation levels (5, 7, and 9 V), and frequencies (20, 25, and 30 Hz). For all these experiments, the mean values of the amplitude of the friction force are calculated using MATLAB. These values are plotted against the corresponding values of input actuator voltage separately according to the voltage applied to the shaker and the frequency of the excitation. The mean amplitudes of the friction force induced by the actuator with varying actuator input voltage are shown in Fig. 11. The maximum actuator voltage that was tested had a level of 120 V. This was the largest voltage that could be applied without the actuator causing the isolator to stick. In other words, the shaker could not provide sufficient force to cause the isolator to move. If the data in Fig. 11 is extrapolated, the maximum value of the friction force that can be induced by the friction damper is found to be approximately 85 N for an actuator input voltage of 150 V, which is the maximum voltage that can be applied to the actuator. The stiffness of the system is found to be 1859.5 N/m. In the final experiments that are conducted, the normal force is controlled using dSPACE. The actuator input voltage is increased linearly from 0 V to 150 in about 10 seconds and after a dwell of 1 second, it is decreased again linearly from 150 V to 0 V. As shown in Fig. 12, the friction force increases linearly with the actuator input voltage.

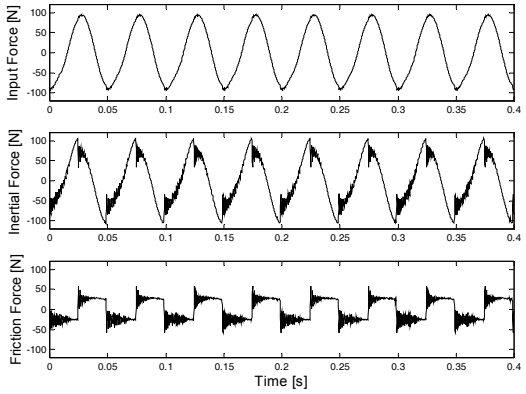


**Fig. 10. Input force, inertial force and the resulting friction force**

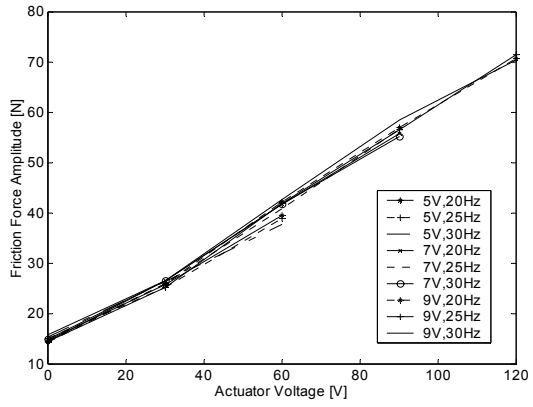


**Fig. 11. Friction force amplitudes at varying excitation amplitudes and frequencies**

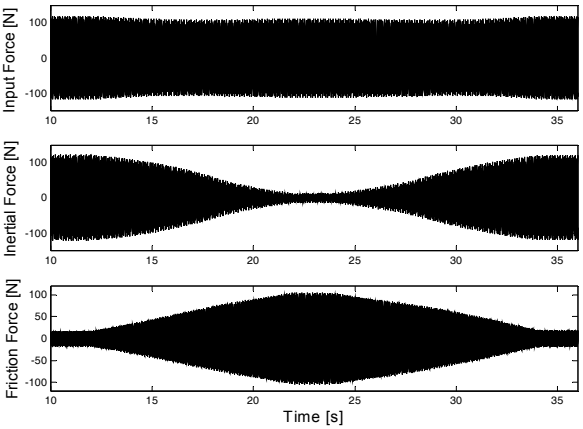


**Fig. 12. Friction force capability of the actuator when the actuator input voltage is varied linearly**

## 5. Conclusions

A new type of semi-active friction-based damper has been developed and has the potential to be used in several active vibration control applications. The heart of the damper is a piezoelectric stack with a mechanical amplifying mechanism. Within this work the frictional force capabilities of the actuator have been characterized experimentally. It was determined that the force generated within the isolator is proportional to the input voltage. Additionally, the maximum force capability of the developed friction damper is approximately 85 N for the specific friction pads used. The stick-slip behavior and the nonlinearities associated with friction make the modeling of this system difficult.

The advantages of the MR damper to the piezoelectric friction damper are that it can achieve a maximum force that is at least 3-4 times larger for a similar size and the manufacturing costs are significantly smaller. The voltage requirements of the MR damper is also much lower. While the friction damper delivers its maximum force at 150 V, a 12 V DC amplifier is sufficient for the MR damper.

The next step in the MR damper is to compare the frequency response of the damper different analytical models to determine which of the models best predict the behavior of the damper. The future work will focus on developing a control scheme based on the model adopted and implementing MR dampers in the connector legs of a parallel platform mechanism to vary the damping of each leg individually. To have an effective range of damping, the inherent friction in the system needs to be kept low and the electromagnet should be capable of delivering a high enough magnetic field.

## 6. Acknowledgment

The authors would like to gratefully acknowledge the support of the U.S. Department of Energy (Grant Number DE-FG04-86NE37967).

## 7. References

[1] S. J. Dyke, B. F. Spencer, M. K. Sain, and J. D. Carlson, "Experimental verification of semi-active structural control strategies using acceleration feedback", *Proceedings of the 3rd International Conference on Motion and Vibration Control*, *Japan*, vol. III, pp. 291-296, 1996.

[2] J. Scruggs and D. Lindner, "Active Energy Control in Civil Structures," *Proceedings of the SPIE - The International Society for Optical Engineering, Newport Beach, CA*, vol. 3671, pp. 194-205, 1999.

[3] J.S. Lane, A.A. Ferri, and B. S. Heck, "Vibration control using semi-active friction damping," *Proceedings of the Winter Annual Meeting of ASME, New York, NY*, vol. 49, pp. 165-171, 1992.

[4] A.A. Ferri and B.S. Heck, "Semi-active suspension using dry friction energy dissipation," *Proceedings of the American Control Conference, Green Valley, AZ*, vol. 1, pp. 31-35, 1992.

[5] S. Kannan., H.M. Uras, and H.M. Aktan, "Active control of building seismic response by energy dissipation*," Earthquake Engineering and Structural Dynamics*, vol. 24, pp. 747-759, 1995.

[6] T.G. Garrett, G. Chen, F.Y. Cheng, and W. Huebner, "Experimental characterization of piezoelectric friction dampers," *Proceedings of the SPIE, New Port Beach, CA*, pp. 405-415, 2001.

[7] G. Chen and C. Chen, "Behavior of piezoelectric friction dampers under dynamic loading," *Proceedings of the SPIE – Smart Structures and Materials, New Port Beach, CA*, vol. 3988, pp. 54-63, 2000.

[8] M.D. Symans and M.C. Constantinou, "Experimental testing and analytical modeling of semi-active fluid dampers for seismic protection," *Journal of Intelligent Material Systems and Structures*, vol. 8, no. 8, pp. 644-657, August 1997.

[9] M.R. Jolly, J.W. Bender, and J.D. Carlson, "Properties and applications of commercial magnetorheological fluids," *Proceedings of SPIE - The International Society for Optical Engineering*, vol. 3327, pp. 262-275, 1998.

[10] M. Yalcintas, "Magnetorheological fluid based torque transmission clutches," *Proceedings of the 1999 9th International Offshore and Polar Engineering Conference*, 1999.

[11] H. Sodeyama, K. Sunakoda, H. Fujitani, S. Soda, N. Iwata, and K. Hata, "Dynamic tests and simulation of magneto-rheological dampers," *Computer-Aided Civil and Infrastructure Engineering,* vol. 18 no. 1, pp. 45-57, January 2003.

[12] R.A. Snyder, G.M. Kamath, and N.M. Wereley, "Characterization and analysis of magnetorheological damper behavior under sinusoidal loading," *AIAA Journal,* vol. 39, no. 7, pp. 1240-1253, July 2001.

[13] G. Yang, B.F. Spencer, J.D. Carlson, and M.K. Sain, "Large-scale MR fluid dampers: Modeling and dynamic performance considerations," *Engineering Structures,* vol. 24, no. 3, pp. 309-323, March 2002.

[14] R. Stanway, J.L. Sproston, and N.G. Stevens, "Nonlinear modeling of an electro-rheological vibration damper," *J. Electrostatics*, vol. 20, pp. 167-184, 1987.